

# Analysis of Metal Transfer and Correlated Influences in Dual-Bypass GMAW of Aluminum

*Various factors, including the welding gun setting, joint penetration, and base metal heat input during this process were examined*

BY Y. SHI, X. LIU, Y. ZHANG, AND M. JOHNSON

**ABSTRACT.** Dual-bypass gas metal arc welding (DB-GMAW) is a modified GMAW process. In this novel process, the base metal current is decreased from the melting current by adding two tungsten electrodes to a conventional GMAW system. The resultant bypass arcs change the forces affecting on the droplet, and the resultant metal transfer becomes more desirable. To understand the desirable changes in the metal transfer, this paper applies established theories to analyze the changes in the forces acting on the droplet and the effects of these changes on the metal transfer behaviors. Analysis shows that the bypass arcs and currents lower the critical current needed to achieve the desired spray transfer. Experimental results obtained by a high-speed camera show that the analysis agrees with experimental data.

## Introduction

Gas metal arc welding (GMAW) is an arc welding process that establishes an arc between a continuously fed consumable metal electrode and the workpiece. Due to its high productivity, it has become one of the predominant methods to join metals. In recent years, more and more aluminum alloy welded structures have been widely applied. The use of aluminum as an alternative material in more applications has brought a higher requirement and challenge to aluminum welding (Ref. 1). As one of the widely used aluminum welding methods, the GMAW process needs improvements in order to achieve higher

weld quality and higher productivity. Since the characteristic of metal transfer in GMAW significantly affects the weld quality especially with respect to its microstructure, porosity formation, strength, and fatigue properties, etc., researchers have made great efforts to study the metal transfer in GMAW (Refs. 2–7). This paper studies the metal transfer in welding aluminum using a novel process that can reduce the heat input.

Low base metal heat input and arc pressure are often critical in meeting specified requirements in aluminum welding (Ref. 8). In a traditional GMAW process, it operates in the globular metal transfer mode at relatively low continuous waveform currents. However, this transfer mode is characterized by periodic formation of large droplets that detach from the electrode primarily by the gravitational force and are typically associated with arc instability (Ref. 9). At higher currents, the transfer mode changes to the desirable spray mode that offers high deposition rate and desirable arc stability, but at the expense of high heat inputs that may be too much for many aluminum welding applications. Moreover, solidification or hot cracking due to the overheating of base metal is also a critical weld quality concern. In order to solve this problem, pulsed gas metal arc welding (GMAW-P) has been developed. In GMAW-P, the pulse parameters can be adjusted to con-

trol the droplet transfer mode, heat input, droplet size, or droplet velocities for different applications. However, to achieve the spray transfer, the peak current has to be greater than the transition current, which is relatively high. This relatively high peak current produces a large arc pressure that can easily generate melt through in complete-joint-penetration applications especially during aluminum welding. Further, the parameters for the pulse waveform need to be determined according to material, shield gas, and wire diameter.

Recently, a modified GMAW process has been developed at the University of Kentucky (Ref. 10) to decouple the melting current (which melts the wire and determines the deposition rate) into the base metal current (which determines base metal heat input and arc pressure) and a bypass current. This process is formed by adding a bypass tungsten electrode to bypass part of the melting current that would otherwise, in conventional GMAW, also flow into the base metal. This modified process is referred to as double-electrode GMAW or DE-GMAW. It can achieve the desirable spray transfer at a wide range of low base metal (continuous-waveform) currents. To further reduce the current needed for the desirable spray transfer to address the need of aluminum welding for low heat input and low arc pressure, the authors have further modified the process to result in dual-bypass GMAW (DB-GMAW) in which two bypass tungsten electrodes are used. Experimental results have indicated that the bypass arcs in DB-GMAW do affect the arc forces and their distribution and consequently affect the metal transfer process. This paper is thus devoted to the analysis of the influences of bypass arcs on the forces acting on the droplet and their influences on metal transfer during DB-GMAW of aluminum.

## KEYWORDS

Dual-Bypass Gas Metal Arc  
Welding (DB-GMAW)  
Current  
Bypass Arcs  
Droplet  
Base Metal Heat Input  
Spray Transfer

Y. SHI is with the State Key Laboratory of Gansu Advanced Nonferrous Metal Materials, Lanzhou University of Technology, Lanzhou, China. Along with X. LIU and Y. ZHANG (ymzhang@engr.uky.edu), SHI is also with the Center for Manufacturing, University of Kentucky, Lexington, Ky. M. JOHNSON is with Los Alamos National Lab, Los Alamos, N.Mex.

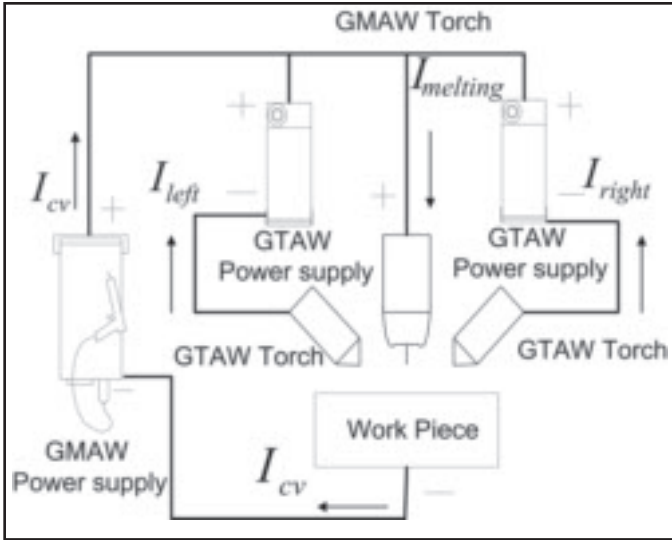


Fig. 1 — Illustration of DB-GMAW.

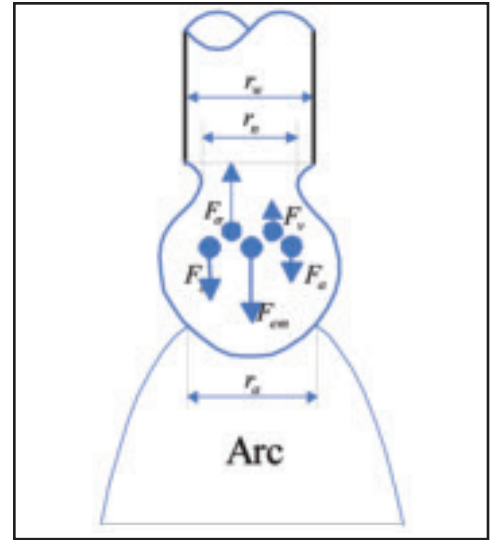


Fig. 2 — Major forces acting on the droplet in GMAW.

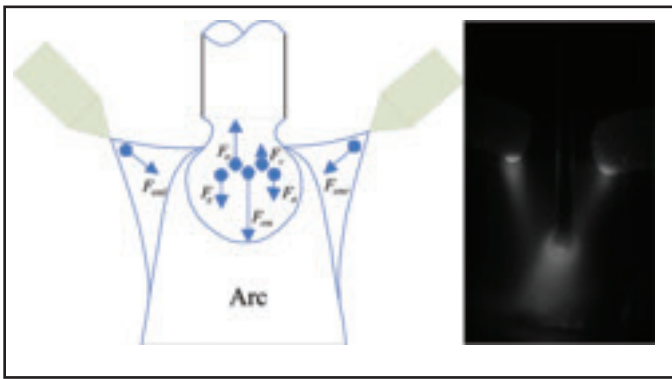


Fig. 3 — Schematic of forces affecting droplet in DB-GMAW.

## Principles of DB-GMAW

A dual-bypass GMAW process shown in Fig. 1 was at the University of Kentucky. As illustrated, the system includes a constant voltage (CV) power supply to provide the base metal current  $I_{cv}$ , and two constant current (CC) power supplies to provide the left and right bypass currents:  $I_{left}$  and  $I_{right}$ . The positive terminals of all three power supplies are connected together to the GMAW gun (which provide the bypass tungsten electrodes), respectively. In this way, the total melting current that melts the wire is the sum of currents, i.e.,  $I = I_{basemetal} + I_{left} + I_{right}$ . Thus, the base metal current that controls the base metal heat input and arc pressure imposed on the base metal can be much less than the total melting current. It has been verified by experiments that the total melting current is determined by the preset wire feed speed (WFS) and the welding voltage

for the CV power supply. Hence, the base metal current can be decreased by increasing the bypass currents because their sum is a constant. Because the bypass currents are provided by two CC power supplies and can be adjusted freely, the DB-GMAW can provide a large range of base metal currents for each set of wire feed speeds and welding voltages to meet

the needs from different applications for different heat inputs and arc pressures. While the effects of DB-GMAW on the base metal heat inputs and arc pressures are straightforward, an analysis is needed in order to understand its effects on the metal transfer process.

## Force Analysis

### Conventional GMAW

Previous research indicates that the type of transfer obtained is determined by the welding current magnitude and polarity, the wire composition, and activation. It also is affected by the wire diameter and wire extension (Ref. 11). The reason that these factors have an impact on metal transfer is because all these parameters can change how the forces act on the droplet.

In conventional GMAW, the major

forces acting on the droplet include the gravity, electromagnetic force (Lorentz force), aerodynamic drag force, surface tension, and vapor jet force (Ref. 12). According to the static-force balance theory (SFBT) (Ref. 3), the balance of these forces determines the metal transfer process, i.e., droplet formation, size, and frequency. These forces are shown in Fig. 2.

The force due to gravity can be expressed as

$$F_g = mg = \frac{4}{3}\pi r_d^3 \rho g \quad (1)$$

where  $r_d$  is the droplet radius,  $\rho$  is the droplet density, and  $g$  is the acceleration of the gravity.

The surface tension is given as (Ref. 12)

$$F_\sigma = 2\pi R\sigma \quad (2)$$

where  $R$  is the electrode radius, while  $\sigma$  is the surface tension coefficient.

The aerodynamic drag force can be expressed as (Ref. 12)

$$F_a = 0.5\pi v_f^2 \rho_f r_d^2 C_d \quad (3)$$

where  $C_d$  is the aerodynamic drag coefficient,  $\rho_f$  and  $v_f$  are the density and fluid velocity of the plasma. This force is higher with higher droplet radius and plasma velocity.

The vapor jet force is given by (Ref. 12)

$$F_v = \frac{m_0}{d_f} IJ \quad (4)$$

where  $m_0$  is the total mass vaporized per second per ampere,  $I$  is the welding current, and  $J$  is the vapor density.

The electromagnetic force,  $F_{em}$ , is given by (Ref. 13)

$$F_{em} = \frac{\mu_0 I^2}{4\pi} \left( \frac{1}{2} + \ln \frac{r_i}{r_u} \right) \quad (5)$$

where  $\mu_0$  is the magnetic permeability,  $I$  is the welding current,  $r_i$  is the exit radius of the current path, and  $r_u$  is the entry radius of the current path. At the time the droplet is initially formed, the radius of the droplet is smaller than the arc radius. At this particular time,  $r_i = r_w$  ( $r_w$  is the radius of the welding wire),  $r_u = r_a$  ( $r_a$  is the radius of anode area). After the appearance of droplet neck,  $r_i = r_n$  ( $r_n$  is the droplet neck radius) and  $r_u = r_a$ .

The balance of the forces on a droplet is given by

$$F_g + F_a + F_{em} = F_\sigma + F_v \quad (6)$$

For spray transfer, Ref. 13 calculated  $F_g$ ,  $F_{em}$ ,  $F_\sigma$ , and  $F_a$  when the welding current is 300 A and the droplet mass is 30 mg. Calculation indicated that the influence from  $F_g$  and  $F_a$  to droplet is relatively smaller;  $F_v$  obviously influences the droplet only under large welding currents (Ref. 12). Therefore, the electromagnetic force is the dominant force facilitating the droplet transfer, and the surface tension is the dominant force retaining the droplet from being transferred. The value of electromagnetic force is exceptionally sensitive to the variation in  $r_a$  (Ref. 13). The electromagnetic force only facilitates the spray when  $r_a$  is larger than  $r_w$ .

## DB-GMAW

The forces in DB-GMAW change significantly from conventional GMAW due to the existence of bypass arcs/currents and the resultant changes in the electromagnetic forces. The two bypass currents that generate  $F_{eml}$  and  $F_{emr}$  are also governed by Equation 5. Assume the bypass currents/arcs are symmetrical and the two bypass currents are equal, then

$$F_{eml} = F_{emr} = \frac{\mu_0 I_{by}^2}{4\pi} \left( \frac{1}{2} + \ln \frac{r_i}{r_u} \right) \quad (7)$$

where  $I_{by}$  is the amperage of the left and right bypass current,  $r_i = r_{byl}$  ( $r_{byl}$  is the bypass arc root radius),  $r_u = r_{by2}$  ( $r_{by2}$  is the bypass arc tip radius). However, due to the change in the direction of the current flow, the direction of the electromagnetic forces generated by the bypass currents changes

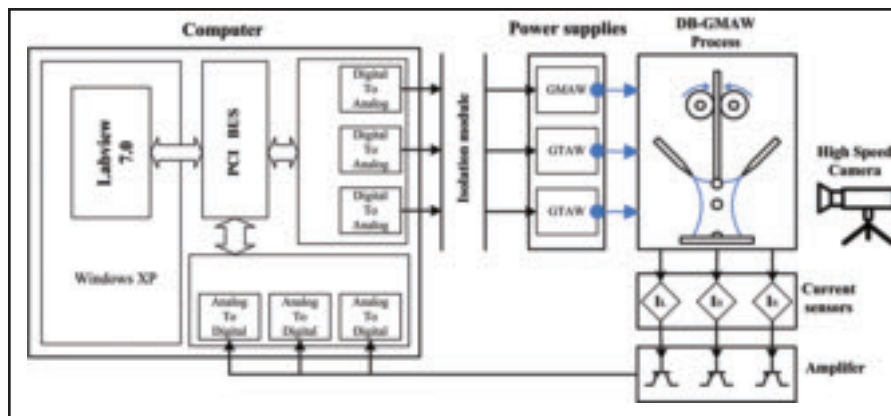


Fig. 4 — Schematic of experimental system.

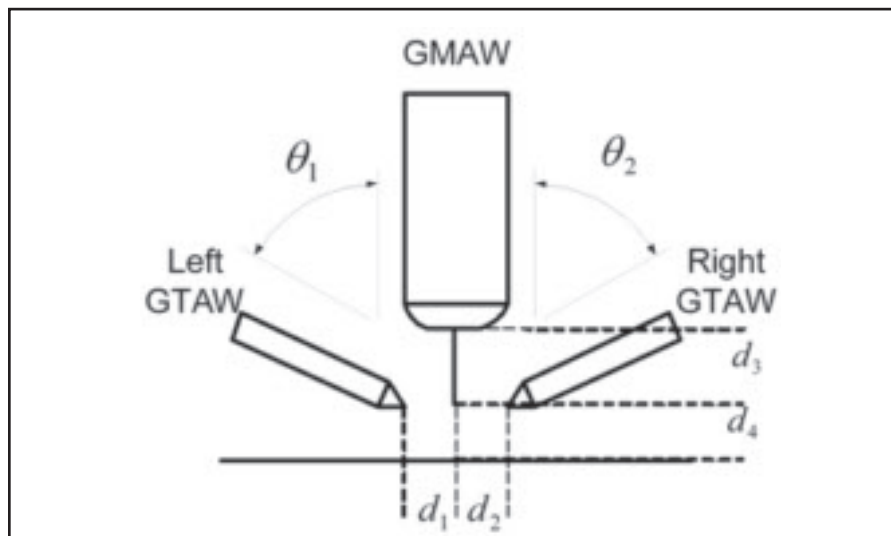


Fig. 5 — Torch installation parameters.

from that of the electromagnetic force in conventional GMAW as shown in Fig. 3.

Due to the direction change, the bypass currents generated electromagnetic forces that can be projected into two directions: along the axis of the electrode and perpendicular to the axis. The components along the electrode axis balance out part of the surface tension. In addition, the perpendicular components of  $F_{eml}$  and  $F_{emr}$  will try to shrink the neck of the droplet so that  $r_u$  should be reduced. As a result, both  $F_{eml}$  and  $F_{emr}$  would tend to increase to accelerate the separation of droplet from the wire.

In addition, bypass arcs would increase the anode area so that the arc root now covers the majority or entire droplet surface — see the differences between Figs. 6, 14. Hence, DB-GMAW increases  $r_a$ ,  $F_{emr}$  and  $F_{eml}$ . As a result, the droplet is easier to transfer than in conventional GMAW.

The bypass arc will facilitate the air

flowing from the upper portion of the droplet to the lower so that the plasma fluid velocity  $V_f$  is increased. According to Equation 3, an increase in  $V_f$  will cause an increase in the aerodynamic drag force  $F_a$ . Although not as dominant as electromagnetic forces,  $F_a$  enhances the detachment of the droplet as well.

The distribution of the forces acting on the droplet in DB-GMAW is shown in Fig. 3. As a result, the introduction of the bypass arcs facilitate the upper part of the droplet in various ways leading to the consequence that the critical current for the spray transfer be decreased from that in conventional GMAW.

## Experimental Procedure

### Experimental System

Figure 4 demonstrates the experimental system that includes a welding system,

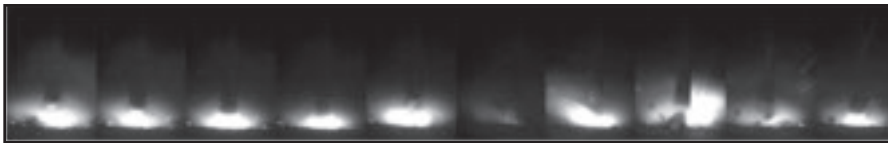


Fig. 6 — Metal transfer without bypass current in Experiment 1. The interval between each frame is 1 ms.

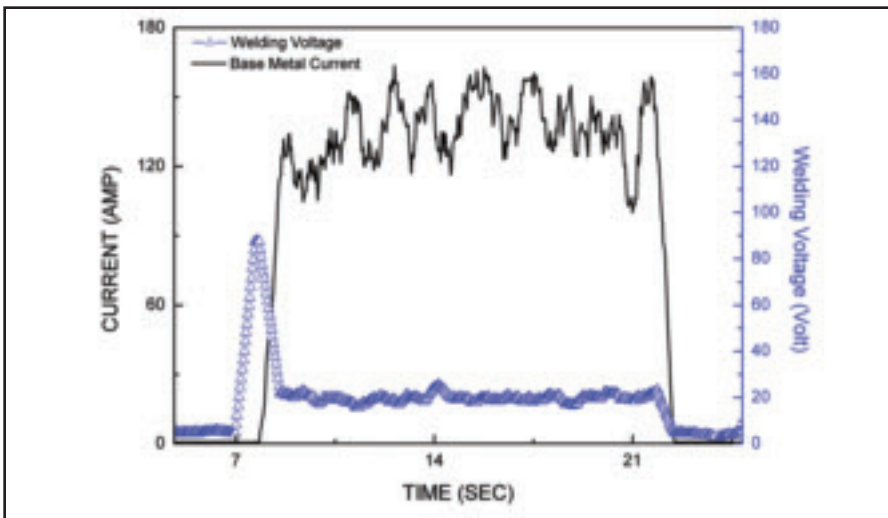


Fig. 7 — Current and voltage in Experiment 1. Bypass currents equal to zero.

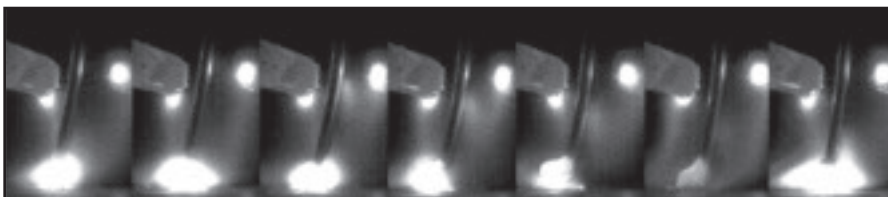


Fig. 8 — Metal transfer with dual 30-A bypass current in experiment 2. The interval between each frame is 2.5 ms.

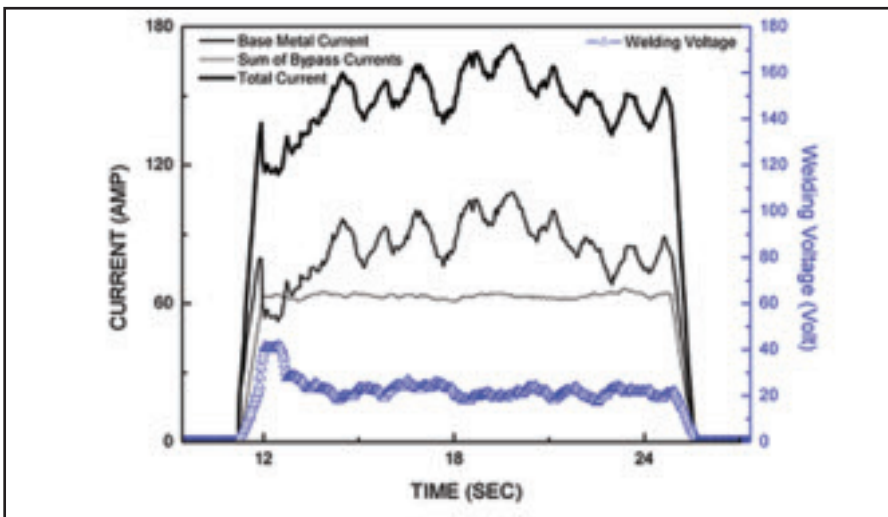


Fig. 9 — Currents and voltages in Experiment 2. Bypass currents equal to 30 A for each.

**Table 1 — Experimental Parameters**

Bypass Current (left and right)

0 A	Experiment 1
30 A	Experiment 2
40 A	Experiment 3
50 A	Experiment 4
60 A	Experiment 5

Constant Parameters

Wire	0.8 mm (0.03 in.) ER 4047
Base metal	Al6061 T6 thickness: 3.2 mm (0.125 in.)
Shielding gas	Pure argon
Gas flow	12 L/min (25.42 ft <sup>3</sup> /h)
Welding speed	240 cm/min (94.5 in./min)
Wire feeding speed	18.6 m/min (733 in./min)
Preset welding voltage	21.5 V
Total welding current	160 A

control system, and sensing system. The welding system is formed by two GTAW torches and one GMAW gun connected to their own power sources, which are two GTAW power supplies and one GMAW power supply. Also, it has a rotation device to rotate the pipe fixed on it. The current (both bypass and base metal) data being monitored by the CLN 500 current sensors is sent to A/D channels of a data acquisition board (PCI-1602). The main arc voltage is also monitored. A high-speed camera is placed horizontally aiming at the GMAW gun to record the metal transfer process. As the major element in the control system, the computer outputs control signals to adjust the bypass currents through the D/A channel during this experiment.

Noise is filtered by a specially designed signal isolation board in order to avoid inaccuracy. LabView 8.2 is adopted in a Windows XP system as the software platform.

Due to the constraint of total current value, the sum of the bypass could not overstep 140 A to ensure the minimum base metal current for the cathode pulverization effect that is the key factor to maintain aluminum GMAW stability.

### DB-GMAW Gun Installation

In the dual-bypass GMAW process, there are three welding arcs: the main arc between the welding wire and the workpiece, the left bypass arc between the welding wire and the left bypass electrode, and the right bypass arc between the welding wire and the right bypass electrode. Here, the welding wire serves as the common anode, and there are three cathodes: the workpiece and the two tungsten elec-

trodes. While the main arc is ensured by the continuous wire feeding, the bypass arcs are ensured by an appropriate setting of the bypass guns.

In order to obtain stable bypass arcs and process, the gun setting must be able to ignite and maintain the bypass arcs easily. To this end, a dual-bypass GMAW gun setting illustrated in Fig. 5 has been developed. It can be seen that it has two GTAW torches symmetrically mounted to the GMAW gun, which is perpendicular to the surface of the workpiece. The two GTAW torches act as the bypass electrodes to pass the bypass currents. All three torches are in the same plane perpendicular to the welding direction.

The tungsten in the bypass GTAW torch can easily emit electrons to ensure the ignition of the bypass arc because of its low electron work function (eV). At the same time, the bypass tungsten electrodes must be close enough to the wire to establish the bypass arcs after the main arc is ignited. To that end, the following geometrical parameters illustrated in Fig. 5 must be set appropriately:

- $d_1$  — Distance from the tip of the left bypass electrode to the wire.
- $d_2$  — Distance from the tip of the right bypass electrode to the wire.
- $d_3$  — Vertical distance from the axis of the GMAW contact tube to the tips of the bypass electrodes.
- $d_4$  — Vertical distance from the tips of the bypass electrodes to the workpiece.
- $\theta_1, \theta_2$  — Angle between left or right bypass torch and GMAW gun, usually 60–70 deg, and  $\theta_1$  always equals to  $\theta_2$ .

Among these parameters,  $d_1, d_2, \theta_1,$  and  $\theta_2$  should be preset, while  $d_3$  and  $d_4$  will be determined by wire feed speed, welding voltage, and electrode extension in welding process. In this experiment, the  $d_1$  and  $d_2, \theta_1$  and  $\theta_2$  were set to 2 mm and 60 deg, respectively. Before every experiment, the wire extension is set as the same length as  $d_3$ .

## Experimental Procedure and Results

Different experiments have been performed using the DB-GMAW process under the parameters shown in Table 1.

Figures 6 and 7 demonstrate the droplet transfer process captured by the high-speed camera and the welding current waveform for Experiment 1 where the bypass current is 0. (The process is thus conventional GMAW.) In this case, as can be seen from Fig. 6, the metal transfer is obviously of short circuit transfer. The droplet grows during the process and transfers itself from the wire tip into the weld pool when it touches the weld pool surface. Spatter is observed.

In Experiment 2, the bypass current in-

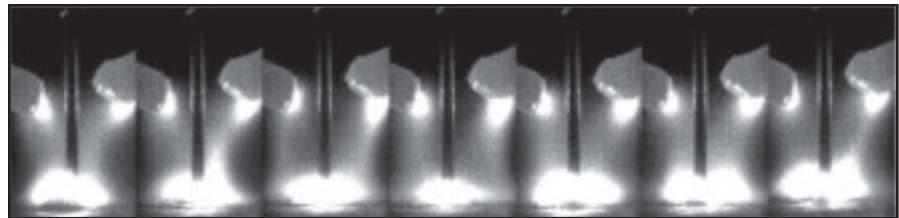


Fig. 10 — Metal transfer with dual 40-A bypass current in Experiment 3. The interval between each frame is 1 ms.

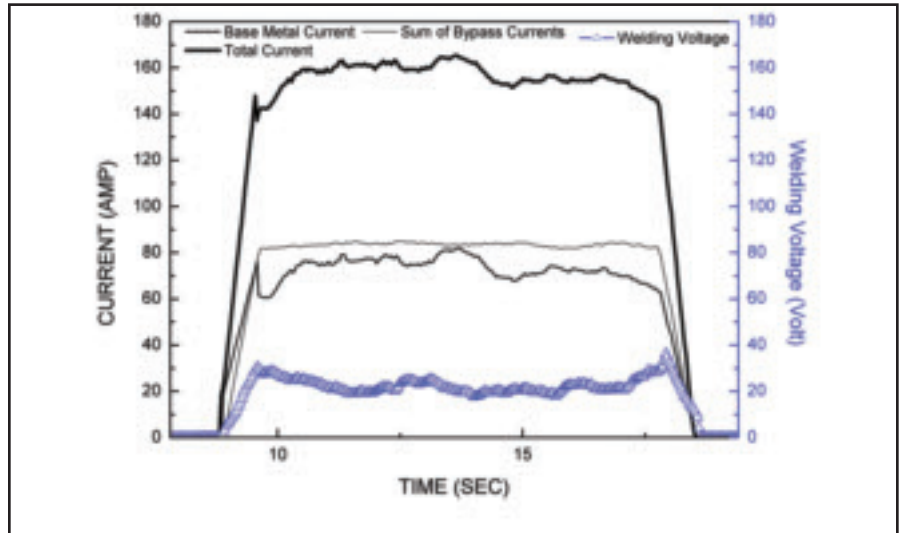


Fig. 11 — Currents and voltage in Experiment 3. Bypass currents equal to 40 A for each.

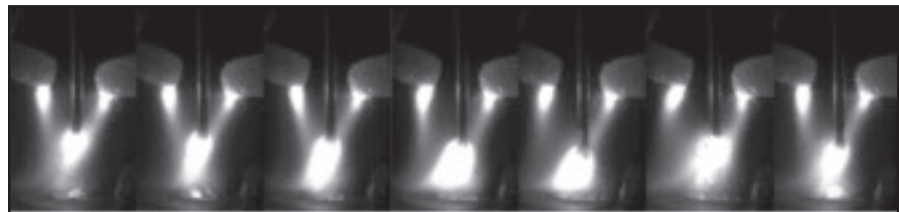


Fig. 12 — Metal transfer with dual 50-A bypass current in Experiment 4. The interval between each frame is 1.5 ms.

creased from 0 to 30 A and the process is truly DB-GMAW. Figures 8 and 9 are the droplet transfer images and welding current waveform, respectively. In this case, the arc length increased but the transfer is still short circuit although the bypass current increased. As can be seen in the images, the droplet keeps increasing before it is transferred into the weld pool; however, it is difficult for the cathode spot to climb from the bottom of the droplet to the wire tip because of the puniness of the bypass arc. In this case, cathode spot force and  $F_{emv}$  would become a resistance that blocks

the droplet from transferring. As long as the droplet keeps growing, the transfer sometimes becomes repelled transfer because of the existence of such resistance. The whole process lacks stability and can lead to undesirable bead shapes.

Figure 10 is the droplet transfer images in Experiment 3 where the bypass current is 40 A. Figure 11 shows the current and voltage waveforms. Observation shows that the droplet size under this parameter is smaller although the droplet transfer is still in a short circuit. In this case, short circuit duration in each period has become

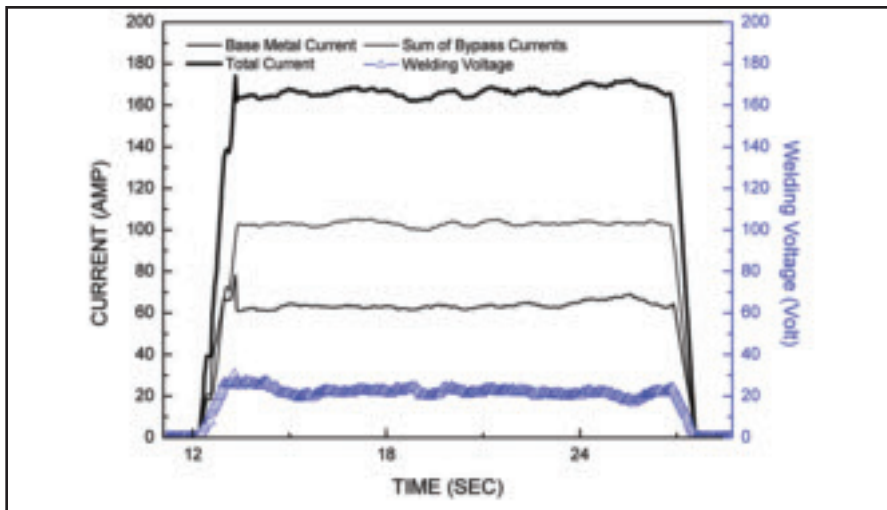


Fig. 13 — Currents and voltage in Experiment 4. Bypass currents equal to 50 A for each.



Fig. 14 — Metal transfer with dual 60-A bypass current in Experiment 5. The interval between each frame is 0.5 ms.

much shorter. This suggests that the metal transfer under this set of parameters is a combination of free transfer and short circuit transfer. Such behavior is very similar to the meso-spray transfer obtained in the aluminum GMAW process. When performing as a combination of free transfer and short circuit transfer, the droplet neck pinching and transfer would be accomplished within a very short time beginning with the moment that the droplet touches the weld pool surface. The process is more stable and leads to better weld beads.

Figure 12 is the droplet transfer images captured when the bypass current is 50 A (Experiment 4). Figure 13 shows the current and voltage waveforms. After the bypass current reached 50 A, the droplet transfer becomes globular free transfer with a very stable process and well-shaped weld beads produced. The arc could climb itself from the bottom of the droplet to the upper during the droplet growing. This makes the droplet transfer resistance forces decrease rapidly. The transfer frequency becomes 150~250 drops/s under such set of parameters. Hence, 50 A of bypass current can be considered as a “criti-

cal” current for the transfer changes from short circuiting to a free transfer in aluminum DB-GMAW when the total current is approximately 160 A.

In Experiment 5, the bypass is further increased to 60 A. The transfer becomes a stable spray transfer as shown in Fig. 14. The current and voltage waveforms in this case are shown in Fig. 15. Observation confirmed that the whole process of droplet growing, neck shrinking, and droplet detaching from the wire tip is quite stable. The frequency of transfer is approximately 400~600 drops/s with uniform droplet size and desirable weld beads produced with no spatters.

All experimental results thus have demonstrated that the droplet transfer mode varies with the parameters. This is caused by the changed forces acting on the droplet, and the change in the bypass current under the same total current is responsible for the force changes. Such results agree with the theoretical analysis in the force analysis section.

Please keep in mind that the purpose of all current and voltage waveforms shown in Figs. 7, 9, 11, 13, and 15 is to briefly

demonstrate the experimental process of Experiments 1~5. Since all these experiments are very stable and parameter fixed during welding, the metal transfer picture captured by a high-speed camera can represent the whole process. It will be difficult correlating the droplet detachment with voltage signal in these figures due to the significant difference of sample rate.

## Influences of DB-GMAW Metal Transfer in Base Metal Heat Input

The metal transfer characteristics of DB-GMAW will certainly bring influences in many aspects such as welding bead profile and base metal heat input.

### Influences on Penetration

The DB-GMAW process has the ability to reduce the arc force acted on the welding pool, which means DB-GMAW can reduce penetration under the same total welding current. The arc force acting on the welding pool can be estimated by Equation 8:

$$F_{arc} = \frac{\mu_0 I^2}{4\pi} \log \left( \frac{r_{bottom}}{r_{top}} \right) \quad (8)$$

$r_{top}$  and  $r_{bottom}$  are radii of the top arc root and bottom arc root, which usually stay steady as long as the process is stable. Since the arc force acting on the welding pool is extraordinary sensitive to base metal current, we can predict that the arc force will significantly decrease in the DB-GMAW process, which would lead to a smaller penetration. Figure 16 demonstrates an experimental verification of the theoretical analysis.

### Influences on Base Metal Heat Input

The DB-GMAW process could also reduce base metal heat input because of its ability to minimize base metal current. In conventional GMAW, radiation from the arc plasma and the weld has only a negligible effect upon the electrode melting rate. Anode, cathode, electrical resistance, and radiation heating have been considered as the sources of heat that conceivably could control the melting rates of welding electrodes (Ref. 14). Anode and cathode heating is directly related to welding current. In DB-GMAW, the contribution of base metal current to the base metal heat input is much smaller than the traditional GMAW process. Thermocouples are used to monitor the base metal heat input during experiments, and the thermal data have provided us significant evidence that DB-GMAW contributed less base metal heat input. The thermocouples are placed on the inner surface of

the workpiece that rotates together with base metal. The thermocouple will go right through the arc column, and the temperature waveform can be recorded by it. Figure 17 indicates the highest temperature waveform from four different processes: two single GMAW processes and two DB-GMAW processes. From Fig. 17, it is obvious to tell that DB-GMAW holds a relatively lower temperature waveform than a single GMAW, which means the base metal heat input is reduced by DB-GMAW under the same welding condition and circumstances.

## Conclusions

1. DB-GMAW decouples the total welding current into bypass currents and base metal current and then controls them separately. This mechanism provides an advantage to reduce the base metal heat input without compromising the wire melting speed and efficiency. As a result, the heat-affected zone (HAZ) and distortion can be reduced in certain applications without affecting the productivity.

2. The bypass arcs significantly affect the forces acting on the droplet that determine the droplet transfer mode:

- The electromagnetic forces generated by the bypass arcs enhance the shrinking of the droplet neck and enlarge the anode area on the bottom of the droplet. The net effect of the neck shrinkage and anode enlargement is to increase the detaching forces.

- The bypass arcs increase the aerodynamic drag force by changing the arc size and plasma flow speed to accelerate the droplet detachment from the wire tip.

The combination of these effects is that the critical current needed to generate the desirable spray transfer is reduced.

3. A series of experiments has been performed to confirm that DB-GMAW indeed has the ability to achieve spray transfer at a lower current than that in conventional GMAW. In addition, it has also been experimentally demonstrated that the metal transfer in DB-GMAW possesses four different modes: short circuiting, globular, meso-spray, and spray transfer. When the total current is given, the transfer mode is determined by the bypass currents or the distribution of the current in three directions: left bypass, base metal, and right bypass.

### Acknowledgment

This work is supported by the Los Alamos National Laboratory (Project No. 4431-001-06), the Natural Science Foundation of China (50675093), and the National Science Foundation (Grant # CMMI-0355324).

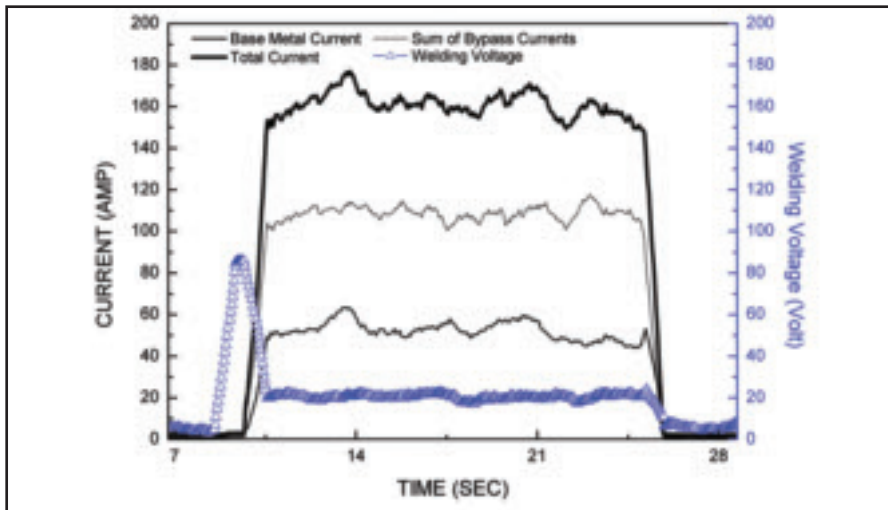


Fig. 15 — Currents and voltage in Experiment 5. Bypass currents equal to 60 A for each.

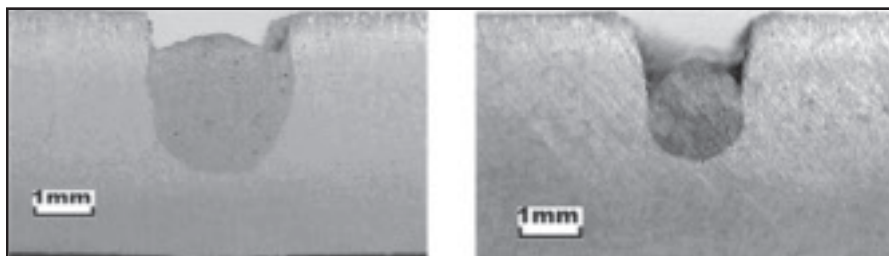


Fig. 16 — Welding cross section of GMAW (left) and DB-GMAW (right) under same welding conditions.

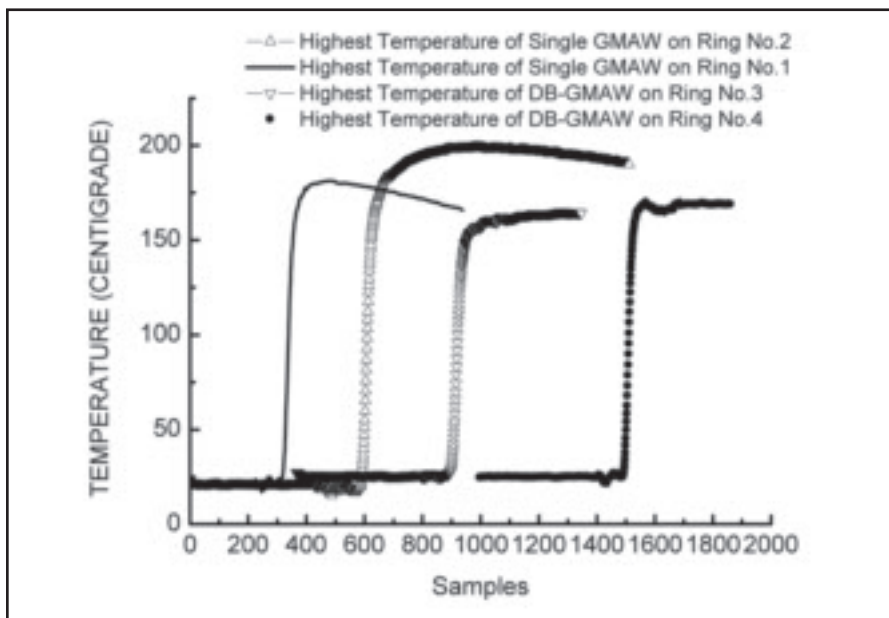


Fig. 17 — Highest temperature comparison on the same workpiece.

## References

1. Merklein, M., and Geiger, M. 2002. New materials and production technologies for innovative lightweight constructions. *Journal of Materials Processing Technology* 45(5): 532–536.
2. Joseph, C., and Benedyk, K. 2000. Light metals in automotive applications. *Light Metal Age* 10(2): 34, 35.
3. Graat, L. H. J., and Waszink, J. H. 1983. Experimental investigation of the forces acting on a drop of weld metal. *Welding Journal* 62(4): 108–116.
4. Kim, Y. S., and Eagar, T. W. 1993. Analysis of metal transfer in gas metal arc welding. *Welding Journal* 72(6): 269–277.
5. Wang, G., Huang, P. G., and Zhang, Y. M. 2004. Numerical analysis of metal transfer in gas metal arc welding under modified pulsed current conditions. *Metallurgical and Materials Transactions B* 35B(8): 857–866.
6. Fan, H. G., and Kovacevic, R. 1999. Droplet formation, detachment, and impingement on the molten pool in gas metal arc welding. *Metallurgical and Materials Transactions B* 30B(8): 791–801.
7. Lin, Q., Li, X., and Simpson, S. W. 2001. Metal transfer measurement in gas metal arc welding. *Journal of Physics D* 4(3): 347–353.
8. Celina, L. M. D. S., and Scotti, A. 2006. The influence of double pulse on porosity formation in aluminum GMAW. *Journal of Materials Processing Technology* 171(Feb.): 366–372.
9. Praveen, P., Yarlagadda, P. K. D. V., and Kangb, M. J. 2005. Advancements in pulse gas metal arc welding. *Journal of Materials Processing Technology* 164-165(May): 1113–1119.
10. Li, K. H., Chen, J. S., and Zhang, Y. M. 2007. Double-electrode GMAW process and control. *Welding Journal* 86(8): 231–237.
11. Lesnewich, A. 1958. Control of melting rate and metal transfer in gas shielded metal-arc welding: Part II — control of metal transfer. *Welding Journal* 37: 418-s to 425-s.
12. Lancaster, J. F. 1984. *The Physics of Welding*. Oxford, England: Pergamon Press.
13. Waszink, J. H., and Piena, M. J. 1986. Experimental investigation of drop detachment and drop velocity in GMAW. *Welding Journal* 65(11): 289–298.
14. Lesnewich, A. 1958. Control of melting rate and metal transfer in gas shielded metal-arc welding: Part I — control of electrode melting rate. *Welding Journal* 37: 343-s to 353-s.

## WELDING JOURNAL

### Instructions and Suggestions for Preparation of Feature Articles

#### Text

- approximately 1500–3500 words in length
- submit hard copy
- submissions via disk or electronic transmission — preferred format is Mac but common PC files are also acceptable
- acceptable disks include zip, CD, and DVD.

#### Format

- include a title
- include a subtitle or “blurb” highlighting major point or idea
- include all author names, titles, affiliations, geographic locations
- separate paper into sections with headings

#### Photos/Illustrations/Figures

- glossy prints, slides, or transparencies are acceptable
- black and white and color photos must be scanned at a minimum of 300 dpi
- line art should be scanned at 1000 dpi
- photos must include a description of action/object/person and relevance for use as a caption
- prints must be a minimum size of 4 in. x 6 in., making certain the photo is sharp
- do not embed the figures or photos in the text
- acceptable electronic format for photos and figures are EPS, JPEG, and TIFF. TIFF format is preferred.

#### Other

- illustrations should accompany article

- drawings, tables, and graphs should be legible for reproduction and labeled with captions
- references/bibliography should be included at the end of the article

#### Editorial Deadline

- January issue deadline is November 21
- February issue deadline is December 19
- March issue deadline is January 23
- April issue deadline is February 20
- May issue deadline is March 23
- June issue deadline is April 20
- July issue deadline is May 22
- August issue deadline is June 22
- September issue deadline is July 24
- October issue deadline is August 21
- November issue deadline is September 21
- December issue deadline is October 22

#### Suggested topics for articles

- case studies, specific projects
- new procedures, “how to”
- applied technology

#### Mail to:

Mary Ruth Johnsen  
Editor, Welding Journal  
550 NW LeJeune Road  
Miami, FL 33126  
(305) 443-9353, x 238; FAX (305) 443-7404  
mjohansen@aws.org